Signals of Deconfinement Phase Transition and Possible Energy Range of Its Detection

K.A. Bugaev[1,*]

[1]*Bogolyubov Institute for Theoretical Physics, NAS of Ukraine, Metrologichna str. 14^B, Kiev 03680, Ukraine*

arXiv:1412.6849v2 [nucl-th] 24 Jan 2015

Abstract

Here we thoroughly discuss the present status of the deconfinement phase transition signals outlined in the NICA White Paper 10.01. It is argued that none of the signals outlined in the NICA White Paper is prepared for experimental verification. At the same time we discuss the new irregularities and new signals of the deconfinement transition found recently within the realistic version of the hadron resonance gas model. All new findings evidence that the mixed quark-gluon-hadron phase can be reached at the center of mass energy of collision 4.3-4.9 GeV.

I. PRESENT STATUS OF TRADITIONAL DECONFINEMENT SIGNALS

After nearly three decades of the heavy ion experiments and the searchers for the quark gluon plasma the situation with the experimental signals of its formation is not clear at the moment. Although some irregularities, widely known as the Kink [1], the Strangeness Horn [2] and the Step [3], were observed and are often attributed to the onset of deconfinement [4], their relation to deconfinement was not clarified. It is necessary to admit that, despite the multiple claims of the authors of Ref. [4] about existence of the statistical model of early stage, in fact, all three above mentioned irregularities cannot be explained within a single framework and, hence, no one exactly understands what these irregularities really signal.

An actual difficulty with a physical interpretation of these irregularities appears due to the fact that up to now they cannot be reproduced either within the transport models like UrQMD and HSD or within the hybrid hydro-cascade models [5]. If in the case of the pure transport models one can always argue that the failure happens due to an absence of the 1-st order phase transition (PT) in these models, this argument does not work for the hybrid hydro-cascade model since in such a model the hydrodynamics is used just to model a PT. Therefore, it is quite possible that we do not understand something very basic at the level of the equation of state with the 1-st order PT. The second possible reason of the hybrid hydro-cascade model failure is that the employed interaction between hadrons is oversimplified. The validity of the last statement was demonstrated very recently by the success of the multicomponent resonance gas model [6] in a simultaneous description of the Strangeness Horn in the ratio of K^+ and π^+ multiplicities and a

*Electronic address: Bugaev@th.physik.uni-frankfurt.de

similar peak in the ratio of Λ and π^- multiplicities. Note that such a model employes different hard-core radii for pions, kaons, all other mesons and that one for baryons [6], which, so far, have not been used in the transport or hybrid hydro-cascade models. Therefore, additional and independent justification of the irregularities suggested in [1–3] is necessary. This task is rather important in view of the planned heavy-ion collision experiments at JINR NICA and GSI FAIR.

It is evident that searching for other irregularities and signals of mixed phase formation and their justification is no less significant. Some efforts to suggest and to discuss new signals of mixed phase formation were made in the NICA White Paper [7]. However, the present situation with the vast majority of deconfinement and /or mixed phase formation signals does not look optimistic. As an example let us briefly consider a situation with a promising signal of the chiral symmetry restoration transition, known as the chiral magnetic effect (CME). Prior to the moment, when local P and CP violations can be included into hydrodynamic, transport and hybrid hydro-cascade models, the situation with the CME physical interpretation as a signal of the chiral symmetry restoration transition will remain unclear. Therefore, all the problems and tasks of future research on CME discussed in the NICA White Paper sections 8.1, 8.2, 8.3 and 8.5 remain actual in the coming years. A similar statement is valid for the chiral vortaic effect discussed in the NICA White Paper section 8.6, i.e. before the P-odd effects are implemented into and studied by hydrodynamic, transport and hybrid hydro-cascade models, it is hard to give a physical interpretation for the chiral vortaic effect.

Hence in this work we critically analyze the typical signals of the deconfinement PT which are outlined in the NICA White Paper 10.01 [7] and discuss their pitfalls. At the same time we present here the new irregularities and new signals of the deconfinement transition found recently within the realistic version of the hadron resonance gas model [6].

II. PHASE TRANSITIONS IN FINITE SYSTEMS AND THE CONCEPT OF SPINODAL PHASE DECOMPOSITION

Due to an absence of the first principle theory of PTs in finite systems the classical, i.e. nonstatistical, models of phase transition become very popular. The typical examples of such models are the usual Van der Waals equation of state and the mean-field models. The main problem with such models is that they do not obey the second and third L. van Hove axioms of statistical mechanics [8, 9]. In particular, in the classical models a PT occurs even at very small number of particles in the system (just a few particles). Such a behavior contradicts to the third axiom of statistical mechanics [8, 9] and to experimental fact that a PT is washed out in a finite system. The major physical reason of these troubles is that the classical models have incorrect parameterization of the gaseous phase neglecting the well known fact that in real systems the gas does not consists just of the molecules, but it consists of the molecule clusters (or droplets)

of all possible sizes [10]. As a consequence, in the mean-field models the mechanisms of phase transition and critical endpoint generation are not realistic and this leads to a contradiction with the L. van Hove axioms of statistical mechanics [8, 9]. Therefore, the conclusions based on such classical models with a PT are not reliable and, hence, they should be verified with the statistical models.

A typical example of the classical model usage in the NICA White Paper is the model of spinodal phase decomposition discussed in the NICA White Paper sections 3.3 and 4.19. The approach outlined in these sections might be interesting for further exploration, but it is dealing solely with the Van der Waals like equation of state. Moreover, it explicitly assumes a concept of uniform matter which during the evolution through the mixed phase region is transformed into the clumps under some additional assumptions and somewhat questionable approximations. Such an approach leads to several principal questions which require a lot of additional work to be done. To be more convincing, it would be nice, if the authors of sections 3.3 and 4.19 provide some additional theoretical arguments and corresponding numerical estimates explaining why in a finite system the isotherms would resemble the isotherms of Van der Waals like equation of state found for an infinite system. So far, this key assumption of sections 3.3 and 4.19 was not throughly justified.

Furthermore, if at the region of the deconfinement PT the quark gluon plasma behaves as the strongly interacting liquid [11], then it is reasonable to assume that the framework of statistical cluster models of liquid-gas 1-st order PT, such as the famous Fisher droplet model [10] of gas condensation, the statistical multifragmentation model [12–14] which describes the nuclear liquid-gas PT, and an exactly solvable statistical model of quark gluon bags with surface tension (QGBST) [15, 16], is better suited to model a deconfinement PT, than any classical equation of state. In these statistical models there is no uniform matter in the mixed phase region. Moreover, one does not need to invent any clumps in this case because within these statistical cluster models the gaseous phase already consists of the clusters of all possible sizes, which in case of the deconfinement PT are the quark gluon plasma bags [17]. Finally, in section 4.19 there is a very interesting observation on the spinodal amplification of density fluctuations at NICA energies. Suppose that an approach of section 4.19 is absolutely correct. Then it would be nice, if the authors of section 4.19 specify how one can detect this spinodal amplification of density fluctuations, because up to now we do not have any method to extract the spatial attenuation of the particle density from the existing experimental data.

A more elaborate approach to study the dynamical aspects of the QCD PTs is based on the nonequilibrium chiral fluid dynamics (the NICA White Paper section 4.20). Its recent development presented in [18] clearly demonstrate that a delay of a PT and interaction between the chiral field and quark-antiquark liquid leads to dissipation and noise, which in turn affect the field fluctuations and lead to the formation of the net baryon density domains [18] which in a sense are similar to clumps. Thus, the present approach can serve as some, but very preliminary, justification for the spinodal phase decomposition discussed in

sections 3.3 and 4.19.

However, even this elaborate approach of the NICA White Paper section 4.20 is not consistent with the exact analytical solutions of such statistical cluster models as the statistical multifragmentation model [19] and the gas of hadronic bags [20] in finite volumes. The authors of sections 3.2 and 4.20 assume that in a finite system the free energy has two local minima which correspond to the macroscopic pure phases, while the mixed phase corresponds to two equal values of free energy of these minima. However, such an assumption is based on the mean-field, i.e. classical equations of state. At the same time, the exactly solvable statistical cluster models [19, 20] tell us that (i) in a finite system the analog of liquid phase may exists at an infinite pressure only, while at finite pressures there can exist only the finite volume analogs of gaseous and mixed phases. Also the models [19, 20] tell us that (ii) in a finite system the gaseous phase always consists of a single state whose free energy is real and it has the minimal value compared to other possible states in a finite system. These other states consist of an even number of metastable states (2, 4, 6 , ... depending on the temperature T and baryonic chemical potential μ) which come in pairs of complex conjugate values of free energy. Then the finite volume analog of a mixed phase consists of a stable gaseous phase and an even number of metastable sates. Moreover, (iii) one can rigorously show that the states which belong to the finite volume analog of mixed phase are not in a true chemical equilibrium with each other, since in finite systems the realistic interaction between hadrons and quark gluons bags differently modifies the chemical potential of each of these states. Therefore, in contrast to the approaches of the NICA White Paper sections 3.2, 3.3, 4.19 and 4.20, in finite systems one has to consider an ensemble of a stable gaseous state and a finite even number of metastable states. Furthermore, it was shown that the imaginary part of the free energy I_n of a metastable state $n = 2, 4, 6, ...$ defines the decay/formation time $t_n \sim 1/|I_n|$ of the n-th state [20]. According to the last formula the gaseous state is always stable since its decay time $t_1 \to \infty$ because $I_1 = 0$. Thus, it seems that the life time of the n-th metastable state in the finite volume analog of mixed phase cannot be taken arbitrarily, but it should depend on the imaginary part of the n-th state free energy. An important question is, however, how can one implement this property into the existing nonequilibrium chiral fluid dynamics?

III. SIGNALS OF THE QCD PHASE DIAGRAM (TRI)CRITICAL ENDPOINT

The situation with the (tri)critical endpoint of the QCD phase diagram is even less clear than with the observed signals of the onset on deconfinement. So far, it is not exactly known whether in our physical world the QCD phase diagram has a critical or a tricritical endpoint. Also up to now there is no first principal definition of the finite volume analog of the (tri)critical endpoint ((tri)CEP). As a results we are forced to use the (tri)CEP definition suited for infinite systems. A typical example of such an approach is

outlined in the NICA White Paper section 3.1, where it is explicitly assumed that in a finite system the (tri)CEP has the same properties as in an infinite system, but with a finite correlation length. Then the whole framework how to possibly detect the (tri)CEP in the experiment is based on such an assumption.

Also in the NICA White Paper section 3.1 it is implicitly assumed that the definition of the correlation length used for static system is correct for an expanding system created in heavy ion collision. However, according to section 4.20 the dynamical study of the correlations and fluctuations is at the very beginning. The usage of the static definition of correlation length in an evolving system is highly non-trivial. Moreover, according to section 4.20 the result for the global correlation length in a finite expanding system depends on the way of the correlation length averaging. Therefore, it seems that in finite non-static systems the (tri)CEP definition via the correlation length is not a reliable one even for the classical model of PT and, hence, we need something more reliable.

Furthermore, the idea to study the multiplicity and p_T spectra fluctuations (p_T is the transversal momentum of secondary hadron) on the event-by-event basis outlined in section 3.1 does not look very optimistic at the moment. Indeed, if the correlation length is finite (and small compared to the typical system size), then very precise measurements are necessary to distinguish the Gaussian and non-Gaussian shapes of the fluctuating quantities. At the moment it is not completely clear whether the existing (and the planned) experimental set-ups are (will be) able to provide the necessary accuracy. Therefore, such estimates are very necessary.

In addition, there are two major difficulties with an interpretation of hadron multiplicities and/or p_T spectra fluctuations.

1. Even in a single collision event the kinetic freeze-out of a given hadron species occurs not at the same thermodynamic parameters, since the different space-time elements of freezing hadron gas have their own thermodynamic parameters at freeze-out. Therefore, the resulting attenuation is already spread over some (not well controlled!) range of the freeze-out temperature T_{fo} and baryonic chemical potential μ_{fo}. Thus, from the very beginning one has to develop a dynamical treatment of fluctuations in a single even of collisions. This is very tough task.

2. The measured hadronic multiplicities and p_T spectra usually contain a sizable contribution of non-thermal hadrons coming from the decay of heavy resonances. According to the NICA White Paper section 4.7 (see also Refs. [85, 86, 88] of this section) in order to get the trustworthy results for hadron multiplicity fluctuations it is absolutely necessary to have a very well defined input of the hadronic mass spectrum including the uncertainty in degeneracy and decay patterns of the high lying resonances, as well as the experiment specific week decays feed-downs. And here there is a principle problem. If the quark gluon bags are, indeed, the highly lying resonances [21], then for a successful

analysis of fluctuations one should include into a treatment all high lying resonances. But then one should also know the above mentioned parameters (degeneracies, decay patterns and so on) of these highly lying resonances which at the moment can only be guessed [22].

Therefore, at the moment one cannot expect that the statistical models with the truncated hadronic mass spectrum can provide us with a reliable information from the experimentally measurable fluctuation patterns for all center of mass energies of collision above 2 GeV. Of course, one can believe that a failure of the statistical hadronization model (or similar models) in describing the experimentally observed fluctuations can be an indirect signal of the quark gluon bags appearing. However, if we need a clear signal, then it will be necessary to work out more realistic, but, consequently, more complicated statistical and transport models which include both the hadronic and quark gluon bag mass spectra.

These general remarks are applicable in full to the net-proton number fluctuations analysis discussed in section 3.10. In addition, an important related task is to elucidate the relation between the net-proton number fluctuations and the existing statistical models with the (tri)CEP and the 1-st order PT of a liquid-gas type [15, 16, 22, 23]. Moreover, in order to understand the meaning of experimentally measured skewness and kurtosis, a similar investigation should be made for the same models, but for finite volumes.

An interesting and important application of the finite size scaling known from spin models to a description of experimental data suggested in [24] allowed one to establish the location of the QCD phase diagram endpoint at the center of mass energy at $\sqrt{s_{NN}} = 47.5$ GeV. This approach also demonstrates that a universality class of the QCD phase diagram endpoint coincides with the one of the 3-dimensional Ising model [24]. However, again no definite conclusion can be made whether this is a critical or a tricritical endpoint. Note that this important issue is simply ignored in the NICA White Paper [7].

IV. NEW IRREGULARITIES AND NEW SIGNALS

Formulation of reliable experimental signals of the deconfinement PT was and is one of the major tasks of heavy ion phenomenology. However, until very recently such efforts were not successful, since they require the realistic equation of state and the model, statistical or dynamical, which is able to accurately describe the existing experimental data and, thus, provide us with reliable information about the late stages of the heavy-ion collision process. Fortunately, the recent improvements [6, 25–27] of the hadron resonance gas model (HRGM) [28–33] provide us with the most successful description of available hadronic multiplicities measured in heavy-ion collisions at AGS, SPS, and RHIC energies. The detailed description of the HRGM and the sets of used experimental data can be found in the original works [6, 25–27], while here we concentrate on its results. The global values of $\chi^2/dof \simeq 1.16$ and $\chi^2/dof \simeq 1.06$ achieved by the

HRGM, respectively, in Refs. [6] and [26] for 111 independent multiplicity ratios measured at 14 values of the center-of-mass energy $\sqrt{s_{NN}}$ = from 2.7 GeV to 200 GeV (more details can be found in [6, 26]). Up to date this is the best quality of the fit achieved by the comparable models. This fact give us a full confidence that the irregularities found in the narrow range of collision energies $\sqrt{s_{NN}} = 4.3 - 4.9$ GeV are not artifacts of the model, but, indeed, they reflect a real situation.

However, the thirty years experience of heavy ion community shows that a formulation of a signal of mixed phase formation is not the most difficult part of the problem, since very many signals were suggested, but only a few of them were observed. The real trouble to formulate a convincing model of the heavy-ion collision process, which would allow one to connect a certain irregularity in the behavior of some observable with the occurrence of the QGP-hadron phase transition. In other words, the hardest part is to verify a suggested signal on the existing theoretical back up and on the existing experimental data.

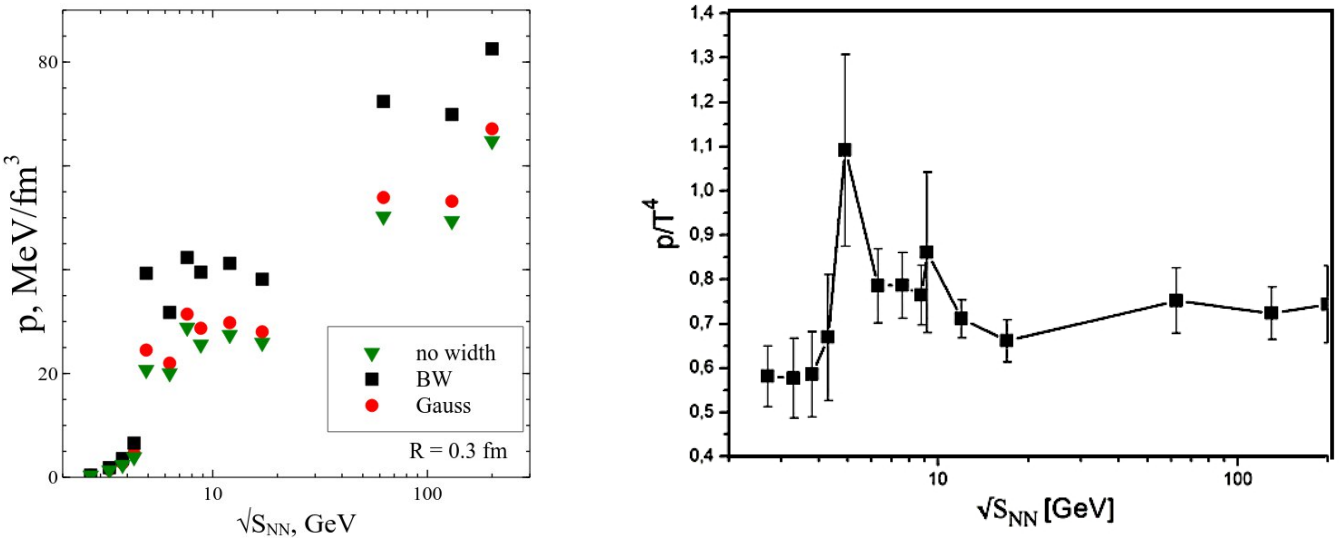

FIG. 1: **Left panel:** Comparison of the chemical FO pressures found within the HRGM with a single hard-core radius for all hadrons [27], but for different parameterizations of the width of hadronic resonances. The Breit-Wigner width parameterization is given by the squares, the Gaussian width is shown by the circles, while a zero width is indicated by the triangles. The results of the HRGM with the multicomponent hard-core repulsion [6] are practically the same. **Right panel:** The number of effective degrees of freedom found for the HRGM with the multicomponent hard-core repulsion [6].

Therefore, our first task was to refine the HRGM and to convert it into a precise tool for obtaining reliable information about the stage of chemical freeze-out (FO). This aim was achieved in Refs. [6, 25–27]. From the left panel of Fig. 1 one can see that the chemical FO pressure p unprecedentedly jumps in 4 - 7 times, depending on the width parameterization for hadronic resonances, if the collision energy $\sqrt{s_{NN}}$ changes from 4.3 GeV to 4.9 GeV. From the right panel of Fig. 1 it is seen that the number of effective degrees of freedom also experiences sizeable increase of about 70% for the model with the multicomponent

hard-core repulsion. This means that the hard-core radii for pions, R_π, kaons, R_K, other mesons, R_m, and baryons, R_b, are different. The best global fit of all hadronic multiplicities was found for $R_b = 0.2$ fm, $R_m = 0.4$ fm, $R_\pi = 0.1$ fm, and $R_K = 0.38$ fm [6]. More details about this version of HRGM can be found in Refs. [6, 25, 26]. It is necessary to stress that all results found within a realistic version of the HRGM with a single hard-core radius of all hadrons are practically the same for the multicomponent version and vice versa, while the unrealistic versions, which correspond to an ideal gas case or the case with hadrons of vanishing width, usually demonstrate somewhat weaker effects.

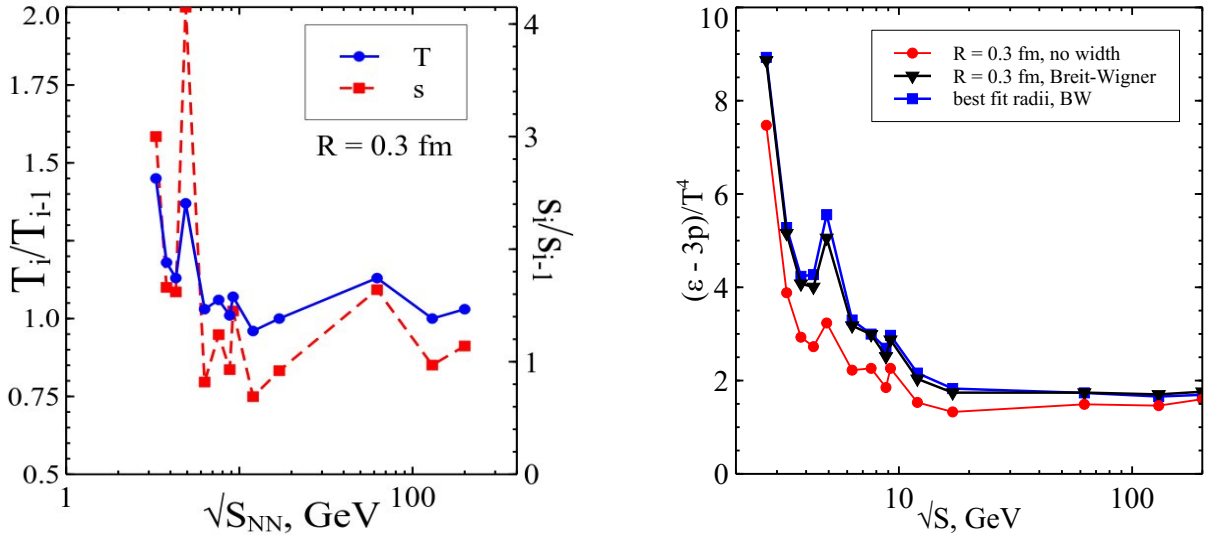

FIG. 2: **Left panel:** Ratio of chemical FO temperatures $T^{FO}(\sqrt{s_{NN}(i)}/T^{FO}(\sqrt{s_{NN}(i-1)})$ and ratio of entropy densities $s^{FO}(\sqrt{s_{NN}(i)}/s^{FO}(\sqrt{s_{NN}(i-1)})$ for two subsequent energies of collision ($i \geq 2$) are shown for the HRGM with the Breit-Wigner width parameterization. For the Gaussian width parameterization the results are practically the same [27]. The lines connected the symbols are given to guide the eyes. **Right panel:** The trace anomaly at chemical FO is shown for the HRGM with a single hard core radius [27] and for the one with the multicomponent hard-core repulsion [6].

Fig. 2 demonstrates other peculiar irregularities at the same energy range $\sqrt{s_{NN}} = 4.3$–4.9 GeV, From the left panel of Fig. 2 it is clearly seen that in this narrow range of collision energy the chemical FO temperature T^{FO} increases in about 1.35 times, while the entropy density at chemical FO in this case jumps in about 4.2 times! Another remarkable irregularity, the behavior of the dimensionless trace anomaly $\delta = \frac{\varepsilon - 3p}{T^4}$, is shown in the right panel of Fig. 2. One may what is the reason for the sharp maxima shown in Fig. 2. Evidently, this irregularities are related to the behavior of the effective number of degrees of freedom, since

$$\delta \equiv T\frac{\partial}{\partial T}\left(\frac{p}{T^4}\right) + \mu_B \frac{\partial}{\partial \mu_B}\left(\frac{p}{T^4}\right) + \mu_{I3}\frac{\partial}{\partial \mu_{I3}}\left(\frac{p}{T^4}\right), \qquad (1)$$

where μ_B is the baryonic chemical potential and μ_{I3} is the chemical potential of the isospin third projection. On the other hand, the entropy density s is a derivative of pressure with respect to temperature, i.e.

$s = \frac{\partial p}{\partial T}$. Therefore, it is not a coincidence that the peak of trance anomaly and the peak of the entropy ratio $s^{FO}(\sqrt{s_{NN}(i)})/s^{FO}(\sqrt{s_{NN}(i-1)})$ occur right at the energy, at which chemical FO pressure has a strong jump.

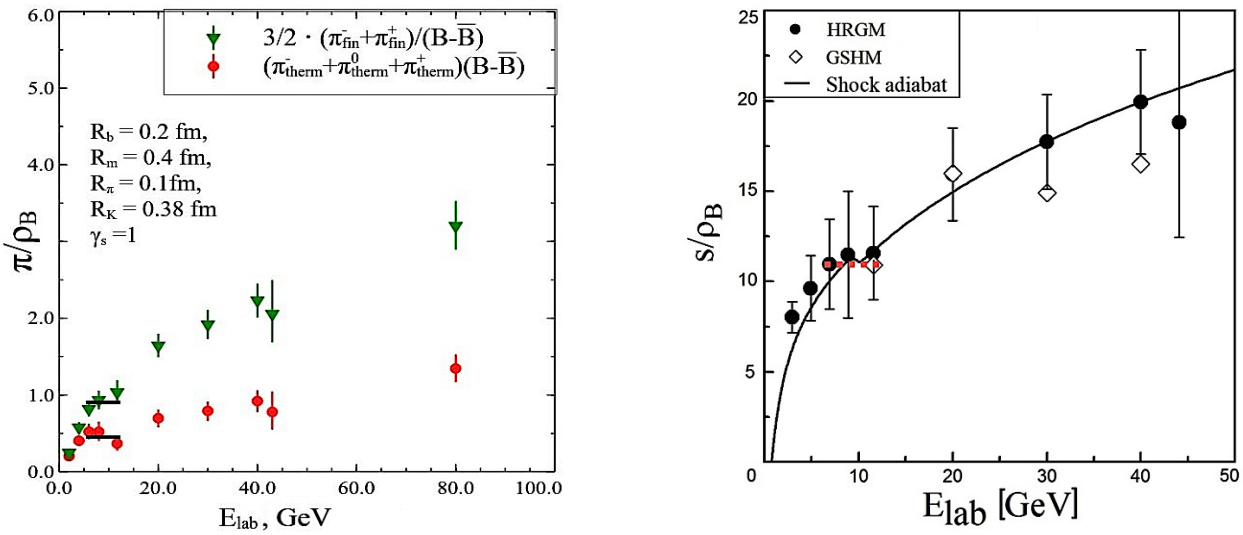

FIG. 3: **Left panel:** The energy dependence of thermal pions per baryon (circles) and the charged pions per baryon (triangle) at chemical FO found for the HRGM with multicomponent repulsion [6]. The horizontal bars indicate the region of correlated plateaus found in the laboratory energy range 6.9–11.6 GeV ($\sqrt{s_{NN}} = 3.8-4.9$ GeV) [34]. **Right panel:** Same as in the left panel, but for the chemical FO entropy per baryon. The circles correspond to the HRGM [6], while the diamonds are shown for the model with chemical nonequilibrium [35]. The dashed horizontal line is the plato correlated with the two plateaus shown in the left panel.

Moreover, a sharp peak in the trace anomaly δ is naturally explained within the shock adiabat model of central nuclear collisions [34] as a formation of the mixed quark-gluon-hadron phase. In Ref. [**?**] it was found that the trace anomaly peak at chemical FO (see Fig. 2) is generated by the corresponding trace anomaly peak on the shock adiabat, which appears at the boundary between the mixed phase and the quark gluon plasma. Therefore, the chemical FO peak of δ is one of the most spectacular signals of deconfinement PT. However, one should keep in mind that for the unrealistic versions of the HRGM (i.e. without hard-core interaction or with a vanishing width of resonances) the δ peak is rather weak (see the right panel of Fig. 2).

The other signal of the deconfinement PT found in [34] is the set of correlated plateaus in the collision-energy dependence of the entropy per baryon, and of the total and the thermal numbers of pions per baryon, which were predicted a long time ago [36–38] to be a manifestation of the anomalous thermodynamic properties of the mixed phase. In fact, these plateaus provide us, probably, with the first deconfinement PT signal which is observed exactly as it was predicted in [36–38]. Only the energy range of this signal estimated in [36–38] is lower because 25 years ago there were no realistic equations of state which could be

thoroughly verified on experimental data available at present. It has to be stressed that the behavior of entropy per baryon found in other models of chemical FO is very similar. This is seen in the right panel of Fig. 3 from the comparison of the HRGM results with the results of the entirely different model developed in [35].

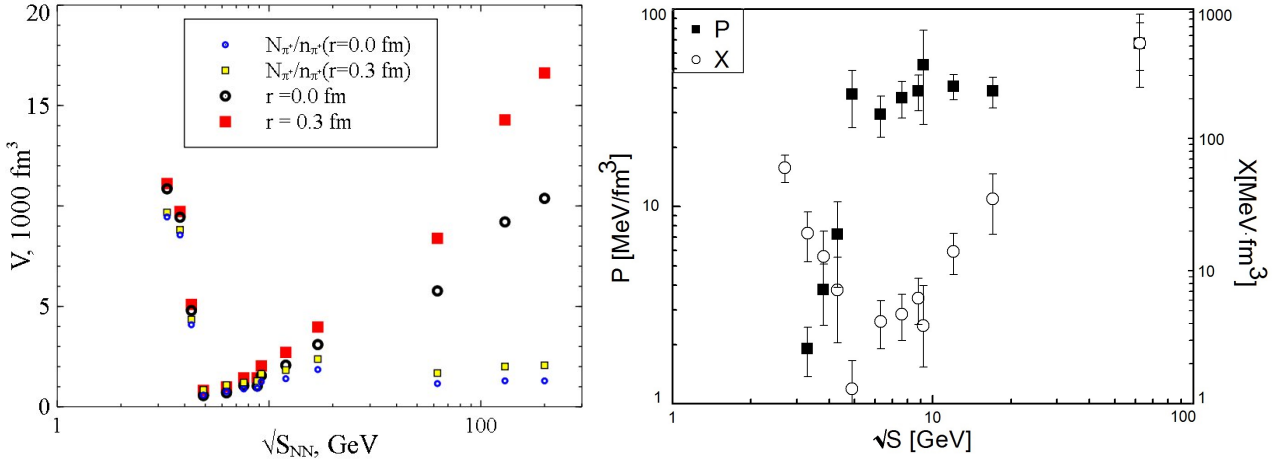

FIG. 4: **Left panel:** The chemical freeze-out volume vs. $\sqrt{s_{NN}}$ for the ideal hadron gas and the hadron gas with the same hard core radius 0.3 fm. The smaller symbols correspond to the fit of hadron yield ratios for the nonstandard set of conservation laws used in [33], while the larger symbols are obtained by the fit of hadron multiplicities with the standard set of conservation laws [25]. In either case there is a local minimum at $\sqrt{s_{NN}} = 4.9$ GeV (or $E_{lab} = 11.6$ GeV). **Right panel:** The relativistic generalized specific volume X (circles) and pressure p (squares) at chemical FO as the functions of collision energy. The minimum of X exists at the same energy $\sqrt{s_{NN}} = 4.9$ GeV as the minimum of the chemical FO volume and jump of the chemical FO pressure.

The numerical simulations of the shock adiabat inside the mixed phase allow one to naturally explain the reason why it was so difficult to pin it down experimentally during last 30 years. The reason is that the whole mixed phase is located within a narrow range of energy (between $\sqrt{s_{NN}} = 3.8$ and $\sqrt{s_{NN}} = 4.9$ GeV, at most, as it is seen from Fig. 3), at which there is a lack of experimental data. At the same time, a good description of the entropy per baryon found at chemical FO within the shock adiabat model (see the solid curve in the right panel of Fig. 3) made it possible to extract the equation of state quark gluon plasma at high baryonic chemical potentials directly from the chemical FO data [34].

Furthermore, the shock adiabat model allowed one to explain an old puzzle of the minimum in the chemical FO volume existing at $\sqrt{s_{NN}} = 4.9$ GeV (see the left panel of Fig. 4). In Refs. [34] it is shown that this minimum is directly related to the minimum of the relativistic generalized specific volume $X \equiv (\varepsilon + p)/\rho_B^2$ which is defined via the pressure p, the energy density ε and the baryinc charge density ρ_B (see the right panel of Fig. 4). Moreover, it is possible to prove [34] that the minimum of X at chemical FO is generated by the X minimum along the shock adiabat existing at the the boundary between the mixed phase and quark gluon plasma.

Thus, all these new irregularities and signals discussed above are thoroughly verified on the existing experimental data and on the chemical FO parameters extracted from the data with the help of the HRGM. Therefore, they make a coherent picture and give us a strong evidence for the deconfinement occurrence at $\sqrt{s_{NN}} = 4.3$–4.9 GeV.

V. CONCLUSIONS

Here we critically discussed the possible signals of deconfinement PT outlined in the NICA White Paper 10.1 and showed that none of these signals is, in fact, worked out yet. Therefore, the weak point of the NICA White Paper is the absence of concrete suggestions what and where to measure in the future experiments to locate the mixed phase.

On the other hand, above we presented a list of concrete observables whose peculiar behavior can serve as the solid foundation for further experimental verification. In fact, the results found recently in [6, 25–27, 34], is a real breakthrough in the problem of formulating the realistic signals of the 1-sf order deconfining transition. They show that the future experiments have a chance to locate the mixed phase, if their accuracy is about an order magnitude better than now, and, if the energy scan steps are about 100 MeV in the laboratory frame.

It is hoped, that the NICA and FAIR Projects together with the BES program at RHIC and the experiments performed at SPS CERN will be able to discover the mixed phase and to experimentally locate the (tri)CEP of QCD phase diagram. It seems, however, that without developing a solid theoretical back up it will be too hard or even impossible to achieve the declared goals.

Acknowledgments. The author is thankful to A. I. Ivanytskyi, D. H. Rischke, E. V. Shuryak, V. D. Toneev and G. M. Zinovjev for fruitful discussions. Important comments of D. B. Blaschke and A. S. Sorin are acknowledged. This publication is based on the research provided by the grant support of the State Fund for Fundamental Research (project N Φ58/175-2014).

[1] M. Gazdzicki, Z. Phys. **C 66**, 659 (1995); J. Phys. **G 23**, 1881 (1997).

[2] M. Gazdzicki and M. I. Gorenstein, Acta Phys. Polon. **B 30**, 2705 (1999).

[3] M. I. Gorenstein, M. Gazdzicki and K. A. Bugaev, Phys. Lett. **B 567**, 175 (2003).

[4] M. Gazdzicki, M.I. Gorenstein and P. Seyboth, Acta Phys. Polon. B **42** (2011) 307.

[5] H. Petersen, J. Steinheimer, G. Burau and M. Bleicher, Eur. Phys. J. C **62** (2009) 31 and references therein.

[6] K. A. Bugaev, D. R. Oliinychenko, A. S. Sorin, G. M. Zinovjev, Eur. Phys. J. A **49**, (2013) 30.

[7] NICA White Paper 10.01 (2014), http://theor.jinr.ru/twiki/pub/NICA/WebHome/WhitePaper 10.01.pdf

[8] L. van Hove, Physica **15**, 951 (1949).

[9] L. van Hove, Physica **15**, 951 (1949). Physica **16**, 137 (1950).

[10] M. E. Fisher, Physics **3**, 255 (1967).

[11] E. V. Shuryak, Prog. Part. Nucl. Phys. **62**, (2009) 48.

[12] J. P. Bondorf et al., Phys. Rep. **257**, (1995) 131.

[13] S. Das Gupta and A.Z. Mekjian, Phys. Rev. C **57**, 1361 (1998).

[14] K. A. Bugaev, M. I. Gorenstein, I. N. Mishustin and W. Greiner, Phys. Rev. **C 62**, (2000) 044320.

[15] K. A. Bugaev, Phys. Rev. **C 76**, (2007) 014903.

[16] K. A. Bugaev, V. K. Petrov and G. M. Zinovjev, Phys. Part. Nucl. Lett. **9**, (2012) 397.

[17] J. I. Kapusta, Phys. Rev. **D 23**, 2444 (1981).

[18] Ch. Herold, M. Nahrgang, I. Mishustin and M. Bleicher, arXive:1304.5372v1.

[19] K. A. Bugaev, Acta. Phys. Polon. **B 36**, (2005) 3083.

[20] K. A. Bugaev, Phys. Part. Nucl. **38**, (2007) 447.

[21] K. A. Bugaev, D. R. Oliinychenko, E. G. Nikonov, A. S. Sorin and G. M. Zinovjev, PoS Baldin ISHEPP XXI (2012) 017, 1-14; arXiv:1212.0132 [hep-ph].

[22] K. A. Bugaev, V. K. Petrov and G. M. Zinovjev, Phys. Rev. **C 79**, (2009) 054913.

[23] K. A. Bugaev, V. K. Petrov and G. M. Zinovjev, Phys. Atom. Nucl. **76**, (2013) 341.

[24] R. A. Lacey, arXiv:1411.7931 [nucl-ex].

[25] D.R. Oliinychenko, K.A. Bugaev and A.S. Sorin, Ukr. J. Phys. **58**, 211 (2013).

[26] K.A. Bugaev et al., Europhys. Lett. **104**, 22002 (2013).

[27] K.A. Bugaev et al., arXiv: 1312.4367v2 (2013).

[28] J. Cleymans and H. Satz, Zeit. Phys. C **57**, 135 (1993).

[29] J. Cleymans, K. Redlich, Phys. Rev. Lett. **81**, 5284 (1998).

[30] P. Braun-Munzinger, I. Heppe, J. Stachel, Phys. Lett. B **465**, 15 (1999).

[31] P. Braun-Munzinger, J. Cleymans, H. Oeschler, K. Redlich, Nucl. Phys. A **697**, 902 (2002).

[32] A. Andronic, P. Braun-Munzinger and J. Stachel, Nucl. Phys. A **772**, 167 (2006) and references therein.

[33] A. Andronic, P. Braun-Munzinger and J. Stachel, Phys. Lett. B **673**, 142 (2009) and references therein.

[34] K. A. Bugaev, A. I. Ivanytskyi, D. R. Oliinychenko, V. V. Sagun, I. N. Mishustin, D. H. Rischke, L. M. Satarov and G. M. Zinovjev, arXiv:1405.3575 [hep-ph]; arXiv:1412.0718 [nucl-th].

[35] J. Letessier and J. Rafelski, Eur. Phys. J. A **35** (2008) 221.

[36] K.A. Bugaev, M.I. Gorenstein, B. Kämpfer and V. I. Zhdanov, Phys. Rev. D **40**, 2903 (1989).

[37] K.A. Bugaev, M.I. Gorenstein and D.H. Rischke, JETP Lett. **52**, 1121 (1990).

[38] K.A. Bugaev, M.I. Gorenstein and D.H. Rischke, Phys. Lett. B **255**, 18 (1991) and references therein.